

[4-(Imidazol-1-yl)thiazol-2-yl]phenylamines. A Novel Class of Highly Potent Colchicine Site Binding Tubulin Inhibitors: Synthesis and Cytotoxic Activity on Selected Human Cancer Cell Lines

Siavosh Mahboobi,^{*,†} Andreas Sellmer,[†] Heymo Höcher,[†] Emerich Eichhorn,[†] Thomas Bär,[‡] Mathias Schmidt,[‡] Thomas Maier,[‡] Josef F. Stadlwieser,[§] and Thomas L. Beckers^{*,‡}

Department of Pharmaceutical Chemistry I, University of Regensburg, D-93040 Regensburg, Germany, and Therapeutic Area Oncology and Enabling Technologies, ALTANA Pharma AG, D-78467 Konstanz, Germany

Received May 10, 2006

Synthesis and cytotoxic activity in the submicromolar range of a series of [4-(imidazol-1-yl)thiazol-2-yl]phenylamines are described. Cell cycle dependent cytotoxicity on RKO human colon carcinoma cells with inducible expression of p27^{kip1} and the influence on microtubule formation were investigated. Considering the significant correlation between the IC₅₀ values of tubulin polymerization inhibition, [³H]colchicine competition, and cytotoxicity of the investigated compounds, tubulin is the main cellular target. The inhibition of microtubule formation was shown to be mediated by interference with the colchicine binding site of tubulin. In depth analysis of the investigated compounds allowed the identification of modifications that altered the pharmacological profile of the compounds from a mitosis-inducing phenotype to a G1 cell cycle arresting phenotype.

Introduction

Within the past decade our understanding of malignant cell growth and the regulation of the cell cycle machinery has offered several new opportunities for targeted cancer therapy and the promise of a broader therapeutic window. Within mitosis, $\alpha\beta$ -tubulin heterodimers building up the mitotic spindle still represent an attractive target for the development of anticancer drugs. Various natural, semisynthetic or fully synthetic new tubulin inhibitors are currently in clinical development like azaepothilone (ixabepilone, Bristol-Myers Squibb) in advanced phase III clinical studies.¹ Another approach in targeted cancer therapy is represented by small-molecule inhibitors of cyclin-dependent kinases (CDKs^a) having a key function in cell cycle regulation.² It is a feature of most cancer cells that they harbor a deregulation of at least one CDK function, making CDK inhibitors particularly attractive as potential therapeutic agents.^{2–4}

In the course of our search for new antimetabolic compounds, we identified compound **1** (Figure 1) from the in-house compound archive as a promising lead. While evaluating the chemical space around this compound, we also investigated structurally related imidazoles of substructure **2** (Figure 1).

Here, we report on the structural refinement of compound **2**, which led to a novel series of highly active antimetabolic, tubulin interfering agents with a [4-(imidazol-1-yl)thiazol-2-yl]phenylamine type structure, inhibiting microtubule polymerization by interfering with the colchicine binding site of β -tubulin.

We further report on analogues with an altered cellular profile shifting from an antimetabolic phenotype to a G1 cell cycle arrest-

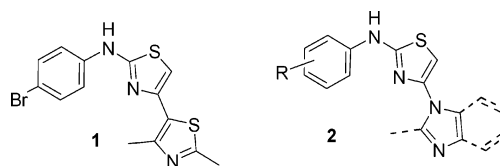


Figure 1. Structure of lead compound 4-bromo[4-(2,4-dimethylthiazol-5-yl)thiazol-2-yl]phenylamine (**1**) and general structure of [4-(imidazol-1-yl)thiazol-2-yl]phenylamines (**2**).

ing phenotype within this series. These compounds were identified during the process of lead optimization by showing distinct new phenotypic alterations in cancer cells. While antimetabolic drugs typically induce a rounding of cells, indicative of mitotic accumulation before the onset of apoptosis, these compounds induced long cell body protrusions typical for inducible expression of CDK inhibitors such as p21^{Waf1} or p27^{Kip1}.

Results and Discussion

Chemistry. According to Scheme 1, the desired [4-(imidazol-1-yl)thiazol-2-yl]phenylamines were prepared from commercially accessible anilines (**3**) employing the strategy of Rasmussen,⁵ which includes formation of *N*-aryl-*N'*-benzoylthioureas (**4**) and debenzoylation to the respective arylthioureas (**5**). After ring closure with ethyl bromoacetate, chlorination of the resulting 2-phenylaminothiazol-4-ones (**6**) with phosphorus oxychloride analogous to Brown et al.⁶ yields (4-chlorothiazol-2-yl)phenylamines (**7**) as intermediates. The desired [4-(imidazol-1-yl)thiazol-2-yl]phenylamines (**8**) were obtained by nucleophilic aromatic substitution in DMF solution, using the respective imidazoles in excess as reagents and bases.

To prepare the corresponding sulfonamides (Scheme 2), a modified synthetic strategy to obtain the 2-phenylaminothiazolin-4-one intermediates **6** was explored. Alkylation of 2-thioxothiazolidin-4-one (**13**) with methyl iodide in aqueous NaOH according to Khodair led to 2-methylsulfanythiazol-4-one (**14**).⁷ The desired 4-(4-oxo-4,5-dihydrothiazol-2-ylamino)benzenesulfonamide (**6j**) was obtained by nucleophilic displacement at C-2 of

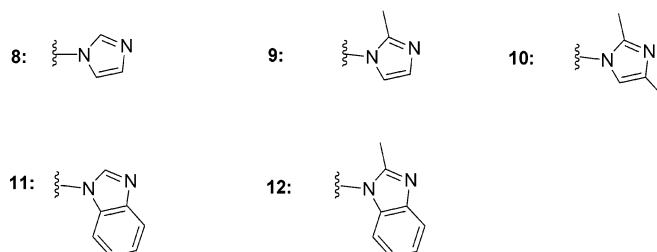
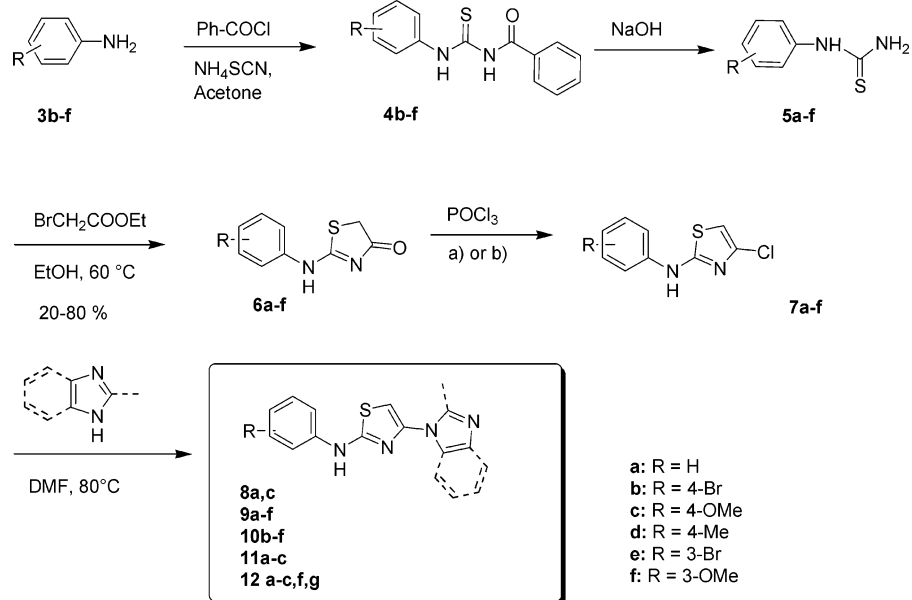
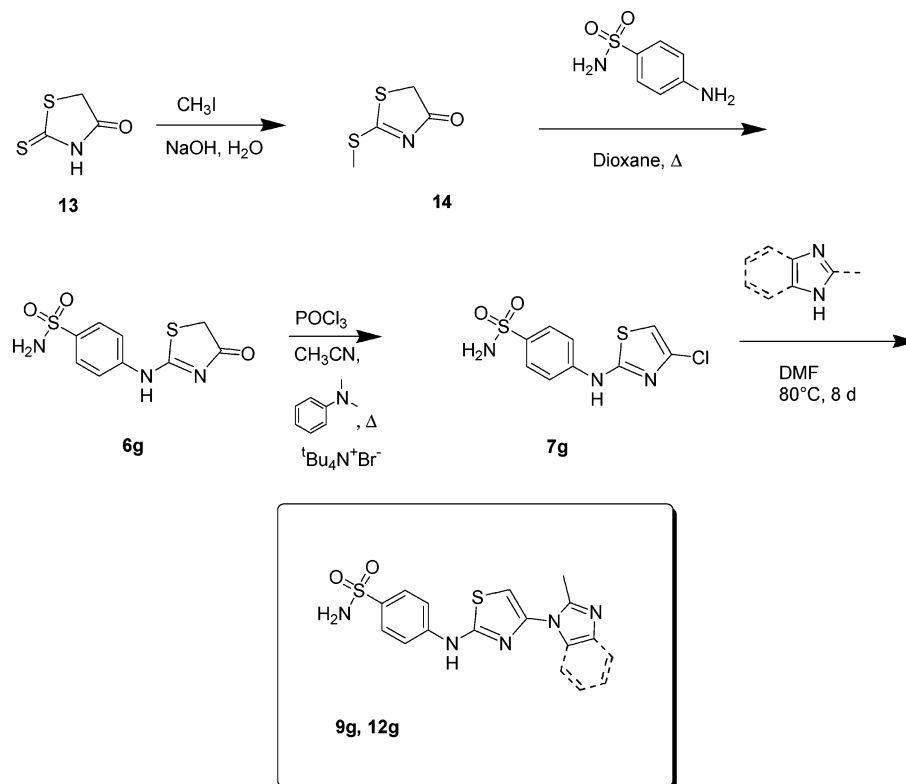
* To whom correspondence should be addressed. For S.M.: phone, (+49) (0) 941-9434824; fax, (+49) (0) 941-9431737; e-mail, siavosh.mahboobi@chemie.uni-regensburg.de. For T.L.B.: phone, (+49) (0) 7531 842974; fax, (+49) (0) 7531 8492974; e-mail, Thomas.Beckers@altanapharma.com.

[†] University of Regensburg.

[‡] Therapeutic Area Oncology, ALTANA Pharma AG.

[§] Enabling Technologies, ALTANA Pharma AG.

^a Abbreviations: CDK, cyclin dependent kinase; G, gap; M, mitosis; MAP, microtubule-associated protein(s); FCS, fetal calf serum; DMEM, Dulbecco's modified Eagle's medium; PBS, phosphate buffered saline; FACS, fluorescence-activated cell sorting.

Scheme 1. Preparation of [4-(imidazol-1-yl)thiazol-2-yl]phenylamines**Scheme 2.** Preparation of [4-(imidazol-1-yl)thiazol-2-ylamino]phenylbenzenesulfonamides

14 by sulfanilamide.⁸ Treatment with phosphorus oxychloride and S_N reaction as described above yielded the desired 4-[4-(imidazol-1-yl)thiazol-2-ylamino]benzenesulfonamides.

Biological Results. Tubulin inhibitors interfere with the M phase of the cell cycle by altering the dynamics of tubulin polymerization, which finally results in the induction of apo-

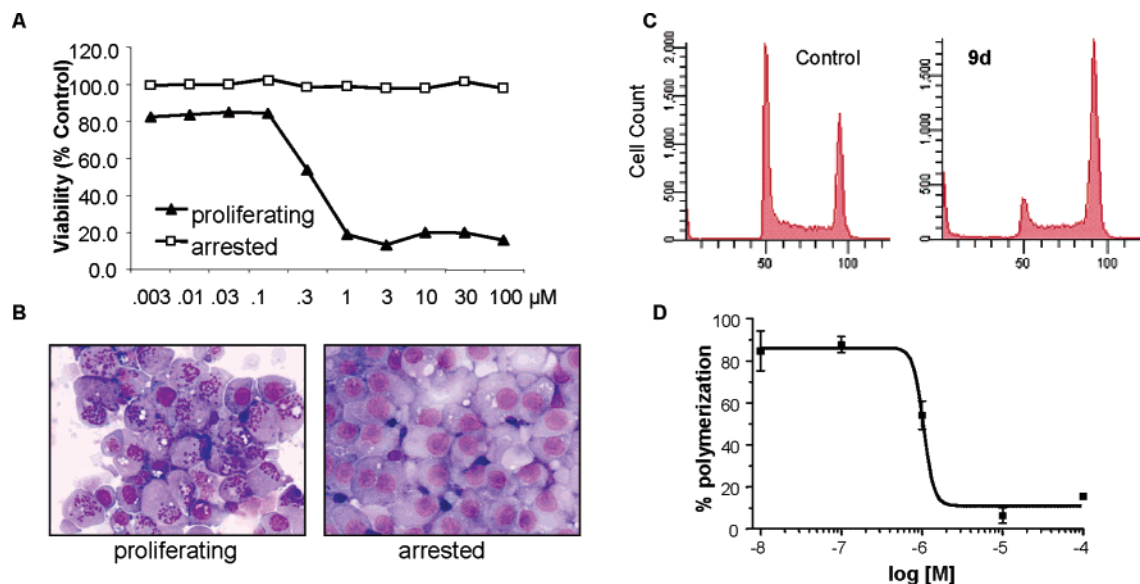


Figure 2. Cell cycle dependent antimetabolic activity of **9d**: (A) determination of the cytotoxicity after 72 h on proliferating (filled triangles) versus arrested (open boxes) RKOp27 cells as described in Experimental Section; (B) methylene blue/eosin staining of proliferating (left) and arrested (right) RKOp27 cells after 24 h of treatment with 10 μM **9d**; (C) cell cycle distribution after treatment with 10 μM **9d**, where control cells (left) were treated with DMSO; 24 h later the cells were harvested, fixed, and stained with propidium iodide as described in Experimental Section prior to analysis by flow cytometry; (D) interference of **9d** with MAP-containing bovine brain tubulin polymerization. The assay was conducted as described in Experimental Section.

Table 1. Structures of **1** and Imidazoles **8–10** and IC_{50} Values on Arrested versus Proliferating RKOp27 Cells^a

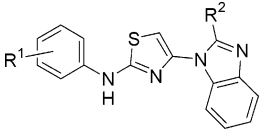
compd	R ₁	R ₂	R ₃	$\text{IC}_{50} \pm \text{SD} (\mu\text{M})$		
				RKOp27 proliferating	RKOp27 arrested	³ H colchicine
1				0.7 \pm 0.1	30 \pm 0	1 \pm 0
8a	H	H	H	> 100 \pm 0	> 100 \pm 0	
9a	H	H	Me	32.5 \pm 2.5	> 100 \pm 0	
10b	4-Br	Me	Me	0.4 \pm 0.1	45 \pm 15	4 \pm 1
9b	4-Br	H	Me	30 \pm 0	> 100 \pm 0	
10c	4-OMe	Me	Me	0.25 \pm 0.05	> 100 \pm 0	7.5 \pm 1.5
9c	4-OMe	H	Me	1.6 \pm 0.4	> 100 \pm 0	8 \pm 2
8c	4-OMe	H	H	> 100 \pm 0	> 100 \pm 0	
10d	4-Me	Me	Me	0.2 \pm 0.05	> 100 \pm 0	6.25 \pm 0.75
9d	4-Me	H	Me	0.45 \pm 0.15	> 100 \pm 0	0.75 \pm 0.45
9g	4-SO ₂ NH ₂	H	Me	49 \pm 1	> 100 \pm 0	
10e	3-Br	Me	Me	> 100 \pm 0	> 100 \pm 0	
9e	3-Br	H	Me	> 100 \pm 0	> 100 \pm 0	
10f	3-OMe	Me	Me	22.5 \pm 7.5	60 \pm 0	
9f	3-OMe	H	Me	22.5 \pm 7.5	> 100 \pm 0	
colchicine				0.016	> 5	0.5 \pm 0.2
podophyllotoxin				0.029	> 0.5	4

^a For selected compounds, the IC_{50} values for [³H]colchicine competition are also given. Values are the average of two independent experiments \pm SD conducted in triplicate (colchicine competition) or quadruplicate samples for each concentration.

ptosis within mitosis. For evaluation of a mitosis-dependent mode of action, the compounds were tested in the genetically engineered human colon carcinoma cell line RKOp27 with ponasterone-A-inducible expression of the cell division cycle kinase inhibitor p27^{kip1}.^{9,10} Induction of p27^{kip1} arrests proliferating RKO cells in the G1 phase of the cell division cycle, thereby inducing complete resistance to antimetabolic agents such as paclitaxel as a stabilizing compound or vincristine as destabilizing tubulin inhibitor.¹

We utilized the RKOp27 system to test the cell cycle dependent cytotoxicity of the compounds described herein. A number

of derivatives tested displayed a significant cell cycle dependent cytotoxicity down to the low micromolar level on proliferating cells and were up to 3000-fold less active in arrested cells. The exemplary cell cycle-dependent activity of **9d** is shown in Figure 2A. Proliferating cells were arrested in mitosis with randomly separated condensed chromosomes (Figure 2B). Flow cytometric analysis to measure the DNA content of proliferating cells confirmed that the majority of cells were arrested in the G2/M stage of the cell cycle (Figure 2C). Since β -tubulin is a prime target for many compounds with antimetabolic mode of action, we investigated the potential interference with microtubule

Table 2. Structures of Benzimidazoles **11** and **12** and Their IC₅₀ Values (Cytotoxicity) on Arrested versus Proliferating RKOp27 Cells^a


compd	R ¹	R ²	IC ₅₀ ± SD (μM)		
			RKOp27 proliferating	RKOp27 arrested	3H colchicine
11a	H	H	>100 ± 0	>100 ± 0	
12a	H	Me	40 ± 0	50 ± 0	
12c	4-OMe	Me	0.025 ± 0.005	52.5 ± 2.5	0.75 ± 0.05
11c	4-OMe	H	>100 ± 0	>100 ± 0	
12f	3-OMe	Me	40 ± 10	60 ± 0	
12b	4-Br	Me	0.09 ± 0.07	60 ± 0	1.25 ± 0.25
11b	4-Br	H	>100 ± 0	>100 ± 0	100 ± 0
12e	3-Br	Me	36 ± 14	85 ± 5	
12g	4-SO ₂ NH ₂	Me	45 ± 5	95 ± 5	

^a For selected compounds, the IC₅₀ values for [³H]colchicine competition are also given. Values are the average of two independent experiments ± SD conducted in triplicate (colchicine competition) or quadruplicate samples for each concentration.

polymerization. **9d** inhibited the in vitro polymerization of MAP-containing bovine brain tubulin with an IC₅₀ of approximately 1 μM (Figure 2D).

The respective IC₅₀ values of further investigated [4-(imidazol-1-yl)thiazol-2-yl]phenylamines on arrested versus proliferating cells are summarized in Table 1, again emphasizing the profound cell cycle dependent cytotoxic activity.

These IC₅₀ data indicate that minor changes in the substitution pattern have a dramatic impact on potency. It appears evident that R¹ inevitably has to be positioned in the para position. A shift of the substituent to the meta position leads to a dramatic loss of potency and to unspecific cytotoxicity. From the representative results in Table 1, we assumed that electron-donating groups on the phenyl moiety are beneficial, while electron-withdrawing groups like sulfamoyl are detrimental. The presence of methyl substituents on the imidazole turned out to

be mandatory. This is demonstrated in compound **9a**, in which a methyl group in the R³ position leads to moderate activity compared to compound **8a**, which is unsubstituted and completely inactive. A methyl group in the R² position may turn moderate activity into submicromolar activity, as shown for compound **10b**, which is 60-fold more active than compound **9b**. The methoxy derivative **10c** represents the most active compound in these series, exhibiting an IC₅₀ of 0.2 μM. Compound **10b** compares directly to compound **1**, demonstrating the superiority of the imidazole series versus the compounds with a terminal thiazole moiety.

Recognizing that R² = CH₃ at the imidazole ring is beneficial, we also evaluated related benzimidazoles. Annellation generally leads to an increase in activity, as shown in Table 2. The 4-bromo compound **12b**, with an IC₅₀ of 0.02 μM, is 20-fold more active than the corresponding imidazole **10b**. As in the imidazole series, a substituent in para position of the phenyl moiety is mandatory, while meta substituents are not tolerated. In close analogy to the imidazole series, the removal of the methyl group (R²) leads to a complete loss of activity.

To further elucidate the mechanism of interference with microtubule formation, we examined whether selected [4-(imidazol-1-yl)thiazol-2-yl]phenylamines directly bind to β-tubulin. A competition binding assay was employed in which the binding of [³H]colchicine to biotinylated bovine brain tubulin is quantified.¹¹ As depicted in Figure 3B, **10b** is able to bind to the colchicine binding site of β-tubulin with an IC₅₀ value of approximately 3 μM. As summarized in Tables 1 and 2, all compounds with potent cell cycle dependent cytotoxicity also interfered with tubulin by binding to the colchicine site of tubulin. Known colchicine competitive tubulin binders such as podophyllotoxin¹² or the 2-aryloindole D-64131¹³ interfere in this assay with IC₅₀ values of 4 and 0.51 μM, respectively.

Inhibition of tubulin polymerization correlated well with colchicine competition for compounds **9d** (3 versus 0.75 μM), **12b** (1.2 versus 1.25 μM), and **12c** (1.25 versus 0.75 μM). The antimetabolic activity of **10b** was determined by its cell cycle dependent cytotoxicity (Figure 3A) together with its ability to

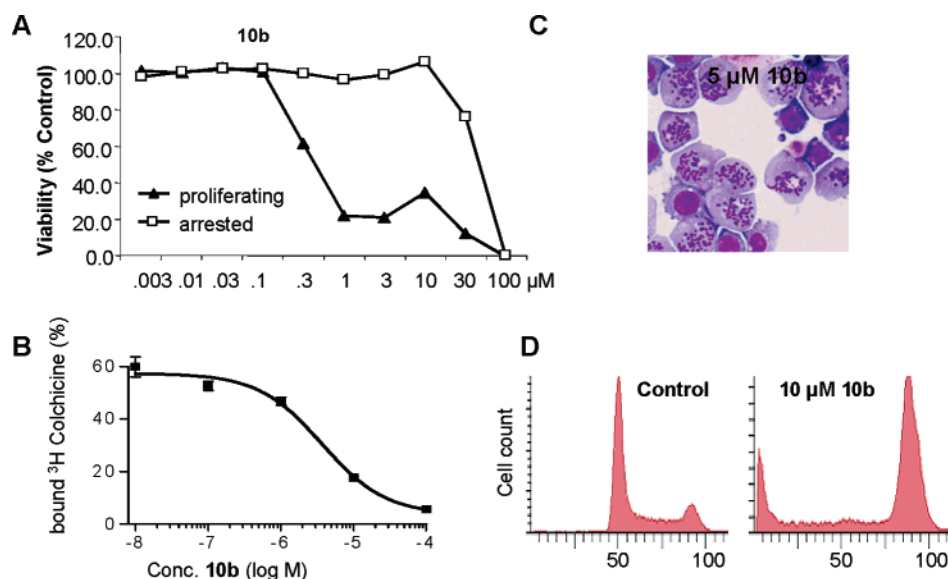


Figure 3. Competition of [³H]colchicine binding to β-tubulin by **10b**. (A) The cell cycle dependent cytotoxicity was determined as described in Figure 2. (B) Competition of [³H]colchicine binding to biotinylated β-tubulin. Various concentrations of **10b** (as indicated) were added, and the IC₅₀ was calculated using Graph Pad Prism software. (C) Methylene blue/eosin staining of RKOp27 cells after 24 h of treatment with 5 μM **10b**. Note the occurrence of a large amount of cells arrested in mitosis. (D) Cell cycle distribution after treatment with 10 μM **9d**. Control cells (left) were treated with DMSO. Treatment was conducted exactly as described in Figure 2 except that A549 human non-small-cell lung cancer cells were used instead of RKOp27 cells. See Experimental Section and the caption of Figure 2 for details.

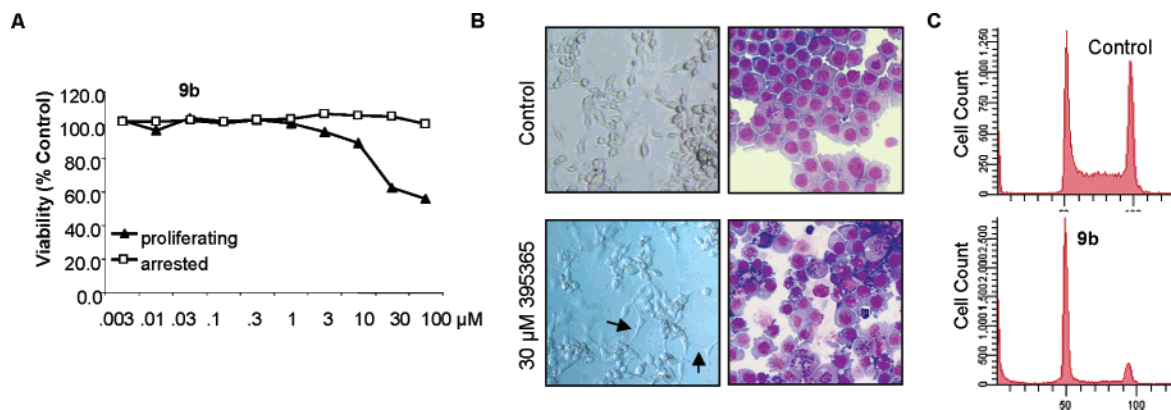


Figure 4. G1 cell cycle arresting properties of **9b**. (A) The cell cycle dependent cytotoxicity was determined as described in Figure 2. (B) Micrographs of RKOp27 cells treated for 72 h with $30 \mu\text{M}$ **9b** (lower left panel). Control cells (upper left panel) were treated with DMSO. Methylene blue/eosin staining of RKOp27 cells was conducted with cells treated for 24 h with $30 \mu\text{M}$ **9b** (lower right panel). Control cells were treated with DMSO (upper right panel). (C) Cell cycle distribution after treatment with $30 \mu\text{M}$ **9b**. The cells were seeded out and treated as indicated in part B. Control cells (upper panel) were treated with DMSO. Twenty-four hours later, the cells were harvested, fixed, and stained with propidium iodide as described in Experimental Section prior to analysis by flow cytometry.

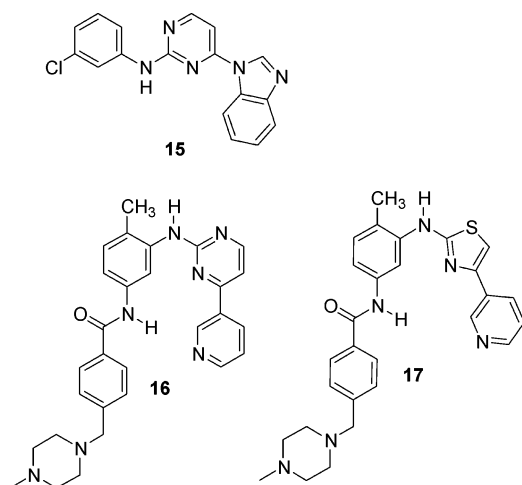


Figure 5. Chemical structures of 3-chloro[4-(benzimidazol-1-yl)pyrimidin-2-yl]phenylamine (**15**), a potent CDK2 inhibitor, imatinib (**16**), and its bioisosteric thiazolyl analogue (**17**).

arrest RKOp27 cells with a large proportion of cells displaying condensed chromosomes (Figure 3C). Cell cycle analyses by flow cytometry confirmed that the majority of the treated cells were arrested in the G2/M phase (Figure 3D)

Interestingly, small modifications changed the cellular profile from a mitosis-confined phenotype to a G1 cell cycle arresting profile. This is exemplified by **9b** (Figure 4), which displayed cell cycle dependent cytotoxicity on RKOp27 cells. However, the potency was much less pronounced and a plateau in viability was reached at about 50% of control cells after 72 h of treatment (Figure 4A). Morphological analysis did not show signs of cytotoxicity (Figure 4B, lower left panel). Moreover, an intriguing change in the morphological shape of RKOp27 cells was observed with the generation of cell body protrusions (indicated by arrows). These morphological alterations were also observed upon inducible expression of cell cycle inhibitors such as p21^{Waf1} or p27^{Kip1} or upon treatment with compounds of CDK inhibitory capacity (data not shown). Similar observations were made with **9a** and **9f**. Methylene blue/eosin staining of treated versus control cells illustrated a slightly increased mitotic index of 8.5%. M-phase cells often displayed abnormal mitosis characterized by condensed chromosomal material that was randomly distributed within the cells. Therefore, it cannot be ruled out that **9b** is still able to interfere with microtubule

polymerization in addition to its G1 arresting capacity. Flow cytometry analyses (Figure 4C) to determine the DNA content confirmed that most of the cells have been arrested in the G1 stage of the cell cycle rather than in mitosis.

Byth et al.^{3,14} previously published a SAR study on several [4-(imidazo[1,2-*a*]pyridine-3-yl)pyrimidin-2-yl]phenylamines as inhibitors of CDK2. In this publication, 3-chloro[4-(benzimidazol-1-yl)pyrimidin-2-yl]phenylamine (**15**) is reported to be a CDK2 inhibitor.

Since bioisosterism¹⁵ between 2-aminopyrimidin and 2-aminothiazole scaffolds is well-known in the field of kinase inhibitors, exemplified by imatinib (**16**)¹⁶ and its thiazolyl analogue **17**^{17,18} (Figure 5), which are both known as c-Kit inhibitors, one may hypothesize that the G1 cell cycle arresting profile of **9b** is related to CDK2 inhibition. Further investigations will be necessary to substantiate the hypothesis, whether small chemical modifications can shift the properties from an optimized microtubule interfering agent to a cell cycle antagonist by inhibition of cyclin-dependent kinase activity or by different mechanistic interactions with the cell cycle machinery.

Conclusion

We describe a novel series of antimitotic, microtubule destabilizing, colchicine-competitive compounds. Starting from a lead identified by high-throughput screening, we were able to rapidly synthesize compounds of a related scaffold, exhibiting cellular activities in the lower nanomolar range. A set of highly active as well as inactive compounds, with only minor structural differences, allowed us to establish a compelling structure–activity relationship. Furthermore, we surprisingly found that minor structural modifications in the investigated inhibitors may also shift the properties from an optimized microtubule interfering agent toward a G1 cell cycle arresting compound.

Experimental Section

Biological Methods. Microtubule Polymerization Assay. The assay was performed as described.¹⁹ For details, see Supporting Information.

Cell Viability Assay. Metabolic activity correlating with cell proliferation/viability was quantified by the Alamar Blue assay as described²⁰ using RKOp27 colon carcinoma cell lines.⁹ For details, see Supporting Information.

Flow Cytometric Analysis. After treatment with test compound, cells were harvested by trypsinization, and an aliquot of 1×10^6 cells was washed once with cold PBS and then fixed with cold

70% ethanol. The DNA was stained with a solution containing 25 $\mu\text{g}/\text{mL}$ propidium iodide and 10 $\mu\text{g}/\text{mL}$ RNase A in PBS for 6 h. Cell cycle distribution was analyzed with a FACScan flow cytometer (Becton Dickinson, San Jose, CA) at an excitation wavelength of 488 nm.

Cell Staining. Upon completion of compound treatment, cells were harvested by trypsinization. An aliquot (5×10^3 cells) was spun onto glass slides using a cytospin and subsequently fixed and stained with the Hemacolor kit (Merck Darmstadt, Germany) according to the manufacturer's instructions.

Colchicine Competition Binding Assay. The assay was conducted basically as described.¹¹ For details, see Supporting Information.

Chemical Procedures. General. NMR spectra were recorded with a Bruker Avance 300 MHz spectrometer at 300 K, using TMS as an internal standard. IR spectra (KBr or pure solid) were measured with a Bruker Tensor 27 spectrometer. Melting points were determined with a Büchi B-545. MS spectra were measured with a Finnigan MAT 95 (EI, 70 eV) with a MAT 710A (CI-MS, NH_3). All reactions were carried out under nitrogen atmosphere. Elemental analyses were performed by the Analytical Laboratory of the University of Regensburg.

4-Bromo[4-(2,4-dimethylthiazol-5-yl)thiazol-2-yl]phenylamine (1). Compound **1** is commercially available at Ambinter Stock Screening Collection, Ambinter, 50 Avenue de Versailles, Paris, F-75016, France; CAS No. 315705-49-8.

Arylthioureas 5b–f were prepared from the corresponding anilines according to the excellent method described by Rasmussen⁵ by debenzoylation of the respective *N*-aryl-*N'*-benzoylthioureas **4b–f**.

Arylaminothiazol-4-ones 6a–f. General Procedure. The arylthioureas **5a–f** (120 mmol) were dissolved in 400 mL of ethanol at 50 °C. To this solution ethyl bromoacetate (156 mmol) was added, and the mixture was stirred at this temperature for 2 h. After cooling to room temperature, the mixture was neutralized with aqueous ammonia. Dropwise addition of water when stirring led to precipitation of the product, which was removed by filtration and dried. Trituration of the resulting solid with petroleum ether (40/60) affords yellow crystals. The title compounds exist as a mixture of tautomers²¹ in DMSO solution. Therefore, the signals in the ¹H NMR spectra are given as observed either in the form of the resulting coalescence spectra or by indicating the proportion in signal intensity for every observable signal.

(2-Phenylamino)thiazol-4-one (6a).²² **6a** was prepared from commercially available phenylthiourea (Acros) as described above. Yield: 5.65 g (82%), yellow crystals. Mp: 178.4–178.5 °C. ¹H NMR (DMSO-*d*₆): δ (ppm) = 11.73 (s, 0.5 \times 1H), 11.15 (s, 0.5 \times 1H), 7.70 (d, 0.5 \times 2H, *J* = 7.4 Hz), 7.40–7.37 (m, 2H), 7.18–7.13 (m, 1H), 7.0 (d, 0.5 \times 2H), 4.01 (s, 0.5 \times 2H), 3.97 (s, 0.5 \times 2H).

(4-Bromophenylamino)thiazol-4-one (6b).²³ **6b** was prepared from 4-bromophenylthiourea (**5b**) as described above. Yield: 7.90 g (67%), beige crystals. Mp: 229–230 °C.²⁴ ¹H NMR (DMSO-*d*₆): δ (ppm) = 11.83 (s, 0.5 \times 1H), 11.28 (s, 0.5 \times 1H), 7.80–7.72 (m, br, 1H), 7.62–7.50 (m, br, 2H), 6.95–6.90 (m, br, 1H), 4.08 (s, 0.5 \times 2H), 4.00 (s, 0.5 \times 2H).

(4-Methoxyphenylamino)thiazol-4-one (6c).²⁵ **6c** was prepared from 4-methoxyphenylthiourea (**5c**) as described above. Yield: 21.45 g (88%), brown crystals. Mp: 178.1–178.2 °C. ¹H NMR (DMSO-*d*₆): δ (ppm) = 11.20 (s, 1H), 7.60 (d, 1H), 6.97–6.93 (m, 3H), 3.96 (s, 0.5 \times 2H), 3.89 (s, 0.5 \times 2H), 3.75 (s, 3H).

(*p*-Tolylamino)thiazol-4-one (6d).²⁶ **6d** was prepared from *p*-tolylthiourea (**6d**) as described above. Yield: 19.85 g (80%), yellow crystals. Mp: 179.2–179.3 °C. ¹H NMR (DMSO-*d*₆): δ (ppm) = 11.33 (s, 1H), 7.56 (d, 0.5 \times 2H), 7.18 (d, 2H), 6.92 (d, 0.5 \times 2H), 3.98 (s, 0.5 \times 2H), 3.92 (s, 0.5 \times 2H), 2.28 (s, 3H).

(3-Bromophenylamino)thiazol-4-one (6e). Preparation from 3-bromophenylthiourea (**5e**) as described above. Yield: 13.42 g (63%), beige crystals. Mp: 177.7–177.8 °C. ¹H NMR (DMSO-

*d*₆): δ (ppm) = 11.58 (s, 1H), 8.37–7.47 (m, br, 1H), 7.33 (s, 2H), 7.21–6.87 (m, br, 1H), 4.00 (s, 2H). Anal. ($\text{C}_9\text{H}_7\text{BrN}_2\text{OS}$) C, H, N.

(3-Methoxyphenylamino)thiazol-4-one (6f).²⁶ **6f** was prepared from 3-methoxyphenylthiourea (**5f**) as described above. Yield: 9.37 g (77%), beige crystals. ¹H NMR (DMSO-*d*₆): δ (ppm) = 11.73 (s, 0.5 \times 1H), 11.13 (s, 0.5 \times 1H), 7.39–7.20 (m, br, 2H), 6.72 (s, br, 1H), 5.57–6.52 (m, br, 1H), 4.00 (s, 0.5 \times 2H), 3.98 (s, 0.5 \times 2H), 3.70 (s, 3H).

4-(4-Oxo-4,5-dihydrothiazol-2-ylamino)benzenesulfonamide (6g) was prepared from **14'** according to the literature.⁸ Yield: 6.50 g (73%), colorless crystals. Mp: 240 °C.²⁷ ¹H NMR (DMSO-*d*₆): δ (ppm) = 11.75 (s, 1H, exchangeable), 7.82 (s, br, 3H), 7.32 (s, 2H exchangeable), 7.10 (s, br, 1H), 4.03 (s, 2H).

(4-Chlorothiazol-2-yl)arylamines 7a–g. General Procedures.

Procedure A. A mixture of the appropriate arylaminothiazol-4-one (4.8 mmol), 3 mL of POCl_3 , and 0.4 mL of pyridine was refluxed for 3 h. After the mixture was cooled to room temperature, the solvent was removed under reduced pressure. The residue was dissolved in ether, and the solution was washed twice with 5% aqueous NaOH, brine, and water. The solvent was dried (Na_2SO_4) and removed under reduced pressure. The crude product was purified by column chromatography.

Procedure B. A mixture of the appropriate arylaminothiazol-4-one (24 mmol), tetrabutylammonium bromide (60 mmol), dimethylaniline (24 mmol), and POCl_3 (144 mmol) in 250 mL of acetonitrile was stirred 5 h at 80 °C. To remove the excess of POCl_3 , water was added carefully at 0 °C. Then an amount of 100 mL of dichloromethane was added, and the organic layer was separated, washed with brine and water, and dried (Na_2SO_4). The solvent was removed under reduced pressure. Purification by column chromatography led to colorless crystals.

(4-Chlorothiazol-2-yl)phenylamine (7a). **7a** was prepared from phenylaminothiazol-4-one (**6a**) according to procedure A. Yield: 3.35 g (32%), colorless crystals. Mp: 96.8–97.4 °C. ¹H NMR (DMSO-*d*₆): δ (ppm) = 10.46 (s, 1H), 7.54 (d, 2H), 7.34 (t, 2H), 7.02 (t, 1H), 6.85 (s, 1H). Anal. ($\text{C}_9\text{H}_7\text{ClN}_2\text{S}$) C, H, N.

(4-Chlorothiazol-2-yl)-4-bromophenylamine (7b). **7b** was prepared from 4-bromophenylaminothiazol-4-one (**6b**) according to procedure B. Yield: 0.22 g (42%), colorless crystals. Mp: 175 °C. ¹H NMR (DMSO-*d*₆): δ (ppm) = 10.60 (s, 1H), 7.53 (m, 4H), 6.90 (s, 1H). Anal. ($\text{C}_9\text{H}_6\text{BrClN}_2\text{S}$) C, H, N.

(4-Chlorothiazol-2-yl)-4-methoxyphenylamine (7c). **7c** was prepared from 4-methoxyphenylaminothiazol-4-one (**6c**) according to procedure B. Yield: 0.90 g (27%), colorless crystals. Mp: 105 °C. ¹H NMR (DMSO-*d*₆): δ (ppm) = 10.25 (s, 1H), 7.46 (d, 2H), 6.93 (d, 2H), 6.78 (s, 1H), 3.72 (s, 3H). Anal. ($\text{C}_{10}\text{H}_9\text{ClN}_2\text{OS}$) C, H, N.

(4-Chlorothiazol-2-yl)-*p*-tolylamine (7d). **7d** was prepared from *p*-tolylaminothiazol-4-one (**6d**) according to procedure B. Yield: 1.05 g (44%), beige crystals. Mp: 114.5 °C. ¹H NMR (DMSO-*d*₆): δ (ppm) = 10.38 (s, 1H), 7.58 (d, 2H), 7.17 (d, 2H), 6.80 (s, 1H), 2.25 (s, 3H). Anal. ($\text{C}_{10}\text{H}_9\text{ClN}_2\text{S}$) C, H, N.

(4-Chlorothiazol-2-yl)-3-bromophenylamine (7e). **7e** was prepared from 3-bromophenylaminothiazol-4-one (**6e**) according to procedure B. Yield: 1.32 g (62%), colorless crystals. Mp: 133 °C. ¹H NMR (DMSO-*d*₆): δ (ppm) = 10.66 (s, 1H), 7.90 (s, 1H), 7.46 (d, 1H), 7.29 (t, 1H), 7.16 (d, 1H), 6.93 (s, 1H). Anal. ($\text{C}_9\text{H}_6\text{BrClN}_2\text{S}$) C, H, N.

(4-Chlorothiazol-2-yl)-3-methoxyphenylamine (7f). **7f** was prepared from 3-methoxyphenylaminothiazol-4-one (**6f**) according to procedure A. Yield: 1.60 g (21%), colorless crystals. Mp: 86–87 °C. ¹H NMR (DMSO-*d*₆): δ (ppm) = 10.47 (s, 1H), 7.26–7.19 (m, 2H), 7.07 (d, 1H), 6.86 (s, 1H), 6.58 (d, 1H). Anal. ($\text{C}_{10}\text{H}_9\text{ClN}_2\text{OS}$) C, H, N.

4-(4-Chlorothiazol-2-ylamino)benzenesulfonamide (7g). **7g** was prepared from 4-(4-oxo-4,5-dihydrothiazol-2-ylamino)benzenesulfonamide (**6g**) according to procedure B. Yield: 3.90 g (66%), colorless crystals. Mp: 165.5 °C (dec). ¹H NMR (DMSO-*d*₆): δ

(ppm) = 10.88 (s, 1H, exchangeable), 7.78 (d, 2H), 7.69 (d, 2H), 7.23 (s, 2H, exchangeable), 6.98 (s, 1H). Anal. (C₉H₈ClN₃O₂S₂) C, H, N.

Synthesis of Target Derivates 8–12. The appropriate (4-chlorothiazol-2-yl)arylamine (3.6 mmol) and the imidazole or benzimidazole derivative (18 mmol) were stirred in 7.5 mL of DMF at 80 °C for 2–8 days (TLC control). The mixture was cooled to room temperature and poured into 300 mL of 5% aqueous Na₂CO₃. The crude product was filtered off, dried, and purified by column chromatography (SiO₂, ethyl acetate) if necessary.

(4-Imidazol-1-ylthiazol-2-yl)phenylamine (8a). **8a** was prepared from (4-chlorothiazol-2-yl)phenylamine (**7a**) and imidazole as described above. Yield: 2.77 g (80%), beige crystals. Mp: 192 °C. ¹H NMR (DMSO-*d*₆): δ (ppm) = 10.51 (s, 1H), 8.28 (s, 1H), 7.75 (s, 1H), 7.64 (d, 2H), 7.36 (t, 2H), 7.08 (s, 1H), 6.97 (m, 2H). Anal. (C₁₂H₁₀N₄S) C, H, N.

(4-Imidazol-1-ylthiazol-2-yl)(4-methoxyphenyl)amine (8c). **8c** was prepared from (4-chlorothiazol-2-yl)-4-methoxyphenylamine (**7c**) and imidazole as described above. Yield: 0.13 g (63%), colorless crystals. Mp: 196 °C. ¹H NMR (DMSO-*d*₆): δ (ppm) = 10.29 (s, 1H), 8.24 (s, 1H), 7.72 (s, 1H), 7.54 (d, 2H), 7.06 (s, 1H), 6.94 (d, 2H), 6.88 (s, 1H), 3.74 (s, 3H). Anal. (C₁₃H₁₂N₄OS) C, H, N.

[4-(2-Methylimidazol-1-yl)thiazol-2-yl]phenylamine (9a). **9a** was prepared from (4-chlorothiazol-2-yl)-4-phenylamine (**7a**) and 2-methylimidazole as described above. Yield: 0.54 g (58%), beige crystals. Mp: 197 °C. ¹H NMR (DMSO-*d*₆): δ (ppm) = 10.49 (s, 1H), 7.61 (d, 2H), 7.46 (s, 1H), 7.34 (t, 2H), 6.98 (t, 1H), 6.92 (s, 2H), 2.49 (s, 3H). Anal. (C₁₃H₁₂N₄S) C, H, N.

(4-Bromophenyl)[4-(2-methylimidazol-1-yl)thiazol-2-yl]amine (9b). **9b** was prepared from (4-chlorothiazol-2-yl)-4-bromophenylamine (**7b**) and 2-methylimidazole as described above. Yield: 0.33 g (60%), beige crystals. Mp: 271 °C. ¹H NMR (DMSO-*d*₆): δ (ppm) = 10.62 (s, 1H), 7.59 (d, 2H), 7.49 (d, 2H), 7.43 (d, 1H), 6.95 (s, 1H), 6.88 (d, 1H), 2.47 (s, 3H). Anal. (C₁₃H₁₁BrN₄S) C, H, N.

(4-Methoxyphenyl)-[4-(2-methylimidazol-1-yl)thiazol-2-yl]amine (9c). **9c** was prepared from (4-chlorothiazol-2-yl)-4-methoxyphenylamine (**7c**) and 2-methylimidazole as described above. Yield: 0.39 g (66%), brown crystals. Mp: 177 °C. ¹H NMR (DMSO-*d*₆): δ (ppm) = 10.27 (s, 1H), 7.52 (d, 2H), 7.41 (s, 1H), 6.92 (d, 2H), 6.87 (s, 1H), 6.81 (s, 1H), 3.73 (s, 3H), 2.47 (s, 3H). Anal. (C₁₄H₁₄N₄OS) C, H, N.

(4-Methylphenyl)-[4-(2-methylimidazol-1-yl)thiazol-2-yl]amine (9d). **9d** was prepared from (4-chlorothiazol-2-yl)-4-methylphenylamine (**7d**) and 2-methylimidazole as described above. Yield: 0.20 g (32%), beige crystals. Mp: 219 °C. ¹H NMR (DMSO-*d*₆): δ (ppm) = 10.37 (s, 1H), 7.48 (d, 2H), 7.41 (s, 1H), 7.13 (d, 2H), 6.87 (s, 1H), 6.85 (s, 1H), 2.47 (s, 3H), 2.25 (s, 3H). Anal. (C₁₄H₁₄N₄S) C, H, N.

(3-Bromophenyl)[4-(2-methylimidazol-1-yl)thiazol-2-yl]amine (9e). **9e** was prepared from (4-chlorothiazol-2-yl)-3-bromophenylamine (**7e**) and 2-methylimidazole as described above. Yield: 0.21 g (43%), beige crystals. Mp: 223 °C. ¹H NMR (DMSO-*d*₆): δ (ppm) = 10.68 (s, 1H), 8.03 (s, 1H), 7.47 (d, 1H), 7.46 (s, 1H), 7.29 (t, 1H), 7.16 (d, 1H), 6.98 (s, 1H), 6.89 (s, 1H), 2.50 (s, 3H). Anal. (C₁₃H₁₁BrN₄S) C, H, N.

(3-Methoxyphenyl)[4-(2-methylimidazol-1-yl)thiazol-2-yl]amine (9f). **9f** was prepared from (4-chlorothiazol-2-yl)-3-methoxyphenylamine (**7f**) and 2-methylimidazole as described above. Yield: 0.28 g (48%), brown crystals. Mp: 179 °C. ¹H NMR (DMSO-*d*₆): δ (ppm) = 10.47 (s, 1H), 7.44 (s, 1H), 7.33 (s, 1H), 7.23 (t, 1H), 7.08 (d, 1H), 6.92 (s, 1H), 6.90 (d, 1H), 6.57 (d, 1H), 3.74 (s, 3H), 2.94 (s, 3H). Anal. (C₁₄H₁₄N₄OS) C, H, N.

4-[4-(2-Methylimidazol-1-yl)thiazol-2-ylamino]benzenesulfonamide Monohydrate (9g). **9g** was prepared from 4-(4-chlorothiazol-2-ylamino)benzenesulfonamide (**7g**) and 2-methylimidazole as described above. Yield: 0.13 g (48%), colorless crystals. Mp: 223.9–225.5 °C. ¹H NMR (DMSO-*d*₆): δ (ppm) = 10.87 (s, 1H), 7.79 (d, 2H), 7.75 (d, 2H), 7.47 (d, 1H), 7.08 (d, 1H, ³J = 1.4 Hz),

7.22 (s, 2H), 7.03 (s, 1H), 6.89 (d, 1H, ³J = 1.4 Hz), 3.49 (s, 3H). Anal. (C₁₃H₁₃N₅O₂S₂·H₂O) C, H, N.

(4-Bromophenyl)[4-(2,4-dimethylimidazol-1-yl)thiazol-2-yl]amine (10b). **10b** was prepared from (4-chlorothiazol-2-yl)-4-bromophenylamine (**7b**) and 2,4-dimethylimidazole as described above. Yield: 0.22 g (22%), beige crystals. Mp: 213 °C. ¹H NMR (DMSO-*d*₆): δ (ppm) = 10.59 (s, 1H), 7.57 (d, 2H), 7.51 (d, 2H), 7.13 (s, 1H), 6.87 (s, 1H), 2.42 (s, 3H), 2.08 (s, 3H). Anal. (C₁₄H₁₃BrN₄S) C, H, N.

(4-Methoxyphenyl)[4-(2,4-dimethylimidazol-1-yl)thiazol-2-yl]amine (10c). **10c** was prepared from (4-chlorothiazol-2-yl)-4-methoxyphenylamine (**7c**) and 2,4-dimethylimidazole as described above. Yield: 0.22 g (35%), beige crystals. Mp: 155.2 °C. ¹H NMR (DMSO-*d*₆): δ (ppm) = 10.22 (s, 1H), 7.51 (d, 2H), 7.10 (s, 1H), 6.91 (d, 2H), 6.72 (s, 1H), 3.72 (s, 3H), 2.42 (s, 3H), 2.07 (s, 3H). Anal. (C₁₅H₁₆N₄OS) C, H, N.

(4-Methylphenyl)[4-(2,4-dimethylimidazol-1-yl)thiazol-2-yl]amine (10d). **10d** was prepared from (4-chlorothiazol-2-yl)-4-dimethylphenylamine (**7d**) and 2,4-dimethylimidazole as described above. Yield: 0.10 g (22%), beige crystals. Mp: 226 °C. ¹H NMR (DMSO-*d*₆): δ (ppm) = 10.31 (s, 1H), 7.48 (d, 2H), 7.13 (d, 2H), 7.10 (s, 1H), 6.76 (s, 1H), 2.42 (s, 3H), 2.25 (s, 3H), 2.08 (s, 3H). Anal. (C₁₅H₁₆N₄S) C, H, N.

(3-Bromophenyl)[4-(2,4-dimethylimidazol-1-yl)thiazol-2-yl]amine (10e). **10e** was prepared from (4-chlorothiazol-2-yl)-3-bromophenylamine (**7e**) and 2,4-dimethylimidazole as described above. Yield: 0.28 g (57%), beige crystals. Mp: 210–213 °C. ¹H NMR (DMSO-*d*₆): δ (ppm) = 10.65 (s, 1H), 8.03 (s, 1H), 7.47 (d, 1H), 7.27 (t, 1H), 7.16 (d, 1H), 7.13 (s, 1H), 6.89 (s, 1H), 2.46 (s, 3H), 2.09 (s, 3H). Anal. (C₂₄H₁₃BrN₄S) C, H, N.

(3-Methoxyphenyl)[4-(2,4-dimethylimidazol-1-yl)thiazol-2-yl]amine (10f). **10f** was prepared from (4-chlorothiazol-2-yl)-3-methoxyphenylamine (**7f**) and 2,4-dimethylimidazole as described above. Yield: 0.18 g (35%), brown crystals. Mp: 172 °C. ¹H NMR (DMSO-*d*₆): δ (ppm) = 10.43 (s, 1H), 7.31 (s, 1H), 7.23 (t, 1H), 7.11 (s, 1H), 7.10 (d, 1H), 6.82 (s, 1H), 6.57 (d, 1H), 3.74 (s, 3H), 2.44 (s, 3H), 2.08 (s, 3H). Anal. (C₁₅H₁₆N₄OS) C, H, N.

4-(Benzimidazol-1-yl)thiazol-2-yl)phenylamine (11a). **11a** was prepared from (4-chlorothiazol-2-yl)phenylamine (**7a**) and benzimidazole as described above. Yield: 1.7 g (82%), beige crystals. Mp: 229 °C. ¹H NMR (DMSO-*d*₆): δ (ppm) = 10.58 (s, 1H), 8.76 (s, 1H), 8.00 (d, 1H), 7.78 (d, 1H), 7.67 (d, 2H), 7.37 (m, 4H), 7.17 (s, 1H), 7.02 (t, 1H). Anal. (C₁₆H₁₂N₄S) C, H, N.

(4-Bromophenyl)[4-(benzimidazol-1-yl)thiazol-2-yl]amine (11b). **11b** was prepared from (4-chlorothiazol-2-yl)-4-bromophenylamine (**7b**) and benzimidazole as described above. Yield: 0.31 g (42%), beige crystals. Mp: 272 °C. ¹H NMR (DMSO-*d*₆): δ (ppm) = 10.72 (s, 1H), 8.77 (s, 1H), 7.97 (d, 1H), 7.78 (d, 1H), 7.67 (d, 2H), 7.53 (d, 2H), 7.35 (m, 2H), 7.21 (s, 1H). Anal. (C₁₆H₁₁BrN₄S) C, H, N.

(4-Methoxyphenyl)[4-(benzimidazol-1-yl)thiazol-2-yl]amine (11c). **11c** was prepared from (4-chlorothiazol-2-yl)-4-methoxyphenylamine (**7c**) and benzimidazole as described above. Yield: 0.22 g (33%), brown crystals. Mp: 214 °C. ¹H NMR (DMSO-*d*₆): δ (ppm) = 10.38 (s, 1H), 8.74 (s, 1H), 7.99 (d, 1H), 7.78 (d, 1H), 7.58 (d, 2H), 7.30–7.43 (m, 2H), 7.08 (s, 1H), 6.97 (d, 2H), 3.75 (s, 3H). Anal. (C₁₇H₁₄N₄OS) C, H, N.

[4-(2-Methylbenzimidazol-1-yl)thiazol-2-yl]phenylamine (12a). **12a** was prepared from (4-chlorothiazol-2-yl)phenylamine (**7a**) and 2-methylbenzimidazole as described above. Yield: 0.28 g (22%), beige crystals. Mp: 130.6 °C (dec). ¹H NMR (DMSO-*d*₆): δ (ppm) = 10.54 (s, 1H, exchangeable), 7.60 (m, 3H), 7.63–7.59 (m, 3H), 7.48–7.43 (m, 3H), 7.34–7.29 (m, 2H), 7.26–7.20 (m, 2H), 7.18 (s, 1H), 6.99–6.95 (m, 1H), 2.60 (s, 3H). Anal. (C₁₇H₁₄N₄S) C, H, N.

(4-Bromophenyl)[4-(2-methylbenzimidazol-1-yl)thiazol-2-yl]amine (12b). **12b** was prepared from (4-chlorothiazol-2-yl)-4-bromophenylamine (**7b**) and 2-methylbenzimidazole as described above. Yield: 0.07 g (12%), beige crystals. Mp: 231 °C. ¹H NMR (DMSO-*d*₆): δ (ppm) = 10.70 (s, 1H), 7.60 (m, 3H), 7.47 (m, 3H), 7.24 (m, 3H), 2.59 (s, 3H). Anal. (C₁₇H₁₃BrN₄S) C, H, N.

(4-Methoxyphenyl)[4-(2-methylbenzimidazol-1-yl)thiazol-2-yl]amine (12c). **12c** was prepared from (4-chlorothiazol-2-yl)-4-methoxyphenylamine (**7c**) and 2-methylbenzimidazole as described above. Yield: 0.06 g (6%), brown crystals. Mp: 171 °C. ¹H NMR (DMSO-*d*₆): δ (ppm) = 10.32 (s, 1H), 7.60 (d, 1H), 7.51 (d, 2H), 7.45 (d, 1H), 7.23 (d, 2H), 7.09 (s, 1H), 6.90 (d, 2H), 3.70 (s, 3H), 2.59 (s, 3H). Anal. (C₁₈H₁₆N₄O₂) C, H, N.

(3-Bromophenyl)[4-(2-methylbenzimidazol-1-yl)thiazol-2-yl]amine (12e). **12e** was prepared from (4-chlorothiazol-2-yl)-3-bromophenylamine (**7e**) and 2-methylbenzimidazole as described above. Yield: 0.57 g (21%), brown crystals. Mp: 241 °C (dec). ¹H NMR (DMSO-*d*₆): δ (ppm) = 10.74 (s, 1H, exchangeable), 8.03–8.01 (m, 1H), 7.65–7.60 (m, 1H), 7.51–7.46 (m, 2H), 7.30–7.23 (m, 4H), 7.16–7.13 (m, 1H), 2.62 (s, 3H). Anal. (C₁₇H₁₃BrN₄S) C, H, N.

(3-Methoxyphenyl)[4-(2-methylbenzimidazol-1-yl)thiazol-2-yl]amine (12f). **12f** was prepared from (4-chlorothiazol-2-yl)-3-methoxyphenylamine (**7f**) and 2-methylbenzimidazole as described above. Yield: 0.05 g (10%), beige crystals. Mp: 106 °C. ¹H NMR (DMSO-*d*₆): δ (ppm) = 10.54 (s, 1H), 7.62 (d, 1H), 7.49 (d, 1H), 7.36 (t, 1H), 7.26–7.21 (m, 3H), 7.18 (s, 1H), 7.07 (d, 1H), 6.55 (d, 1H), 3.70 (s, 3H), 2.61 (s, 3H). Anal. (C₁₈H₁₆N₄O₂) C, H, N.

4-[4-(2-Methylbenzimidazol-1-yl)thiazol-2-ylamino]benzenesulfonamide Hydrochloride Monohydrate (12g). **12g** was prepared from 4-(4-chlorothiazol-2-ylamino)benzenesulfonamide (**7g**) and 2-methylbenzimidazole as described above. Yield: 0.60 g (23%), beige crystals. Mp: 271.1–272.2 °C. ¹H NMR (DMSO-*d*₆): δ (ppm) = 10.95 (s, 1H, exchangeable), 7.78–7.72 (m, 4H), 7.66–7.60 (m, 1H), 7.49–7.44 (m, 1H), 7.30 (s, 1H), 7.27–7.22 (m, 2H), 7.21 (s, 2H, exchangeable), 2.61 (s, 3H). Anal. (C₁₇H₁₅N₅O₂S₂·HCl·H₂O) C, H, N.

Supporting Information Available: Experimental details concerning microtubule polymerization assay, cell viability assay, and colchicine competition binding assay, IR spectral data, EI spectral data, and the results of combustion analysis. This material is available free of charge via the Internet at <http://pubs.acs.org>.

References

- Beckers, T.; Mahboobi, S. Natural, semisynthetic and synthetic microtubule inhibitors for cancer therapy. *Drugs Future* **2003**, *28*, 767–785.
- Swanton, C. Cell-cycle targeted therapies. *Lancet Oncol.* **2004**, *5*, 27–36.
- Byth, K. F.; Cooper, N.; Culshaw, J. D.; Heaton, D. W.; Oakes, S. E.; Minshull, C. A.; Norman, R. A.; Pauptit, R. A.; Tucker, J. A.; Breed, J.; Pannifer, A.; Rowsell, S.; Stanway, J. J.; Valentine, A. L.; Thomas, A. P. Imidazo[1,2-*b*]pyridazines: a potent and selective class of cyclin-dependent kinase inhibitors. *Bioorg. Med. Chem. Lett.* **2004**, *14*, 2249–2252.
- Schwartz, G. K.; Shah, M. A. Targeting the cell cycle: a new approach to cancer therapy. *J. Clin. Oncol.* **2005**, *23*, 9408–9421.
- Rasmussen, C. R.; Villani, F. J.; Weaner, L. E.; Reynolds, B. E.; Hood, A. R.; Hecker, L. R.; Nortey, S. O.; Hanslin, A.; Costanzo, M. J.; Powell, E. T.; Molinari, A. J. Improved procedures for the preparation of cycloalkyl-, arylalkyl-, and arylthioureas. *Synthesis* **1988**, *6*, 456–459.
- Brown, M. L.; Cheung, M.; Dickerson, S. H.; Gauthier, C.; Harris, P. A.; Hunter, R. N.; Pacofsky, G.; Peel, M. R.; Stafford, J. A. Preparation of 1,3-oxazol-2-amines as VEGFR2, CDK2, and CDK4 inhibitors. PCT WO 2004/032882 A2, 2004.
- Khodair, A. I. A convenient synthesis of 2-arylidene-5*H*-thiazolo[2,3-*b*]quinazoline-3,5[2*H*]-diones and their benzoquinolone derivatives. *J. Heterocycl. Chem.* **2002**, *39*, 1153–1160.

- Peciura, R.; Tarasevicius, E.; Martinkus, R.; Sosnovskaya, A. Antituberculous activity of new 2-and 5-substituted Δ²-thiazolin-4-ones. *Pharmazie* **1981**, *36*, 862–863.
- Schmidt, M.; Lu, Y.; Liu, B.; Fang, M.; Mendelsohn, J.; Fan, Z. Differential modulation of paclitaxel-mediated apoptosis by p21^{waf1} and p27^{kip1}. *Oncogene* **2000**, *19*, 2423–2429.
- Schmidt, M.; Lu, Y.; Parant, J. M.; Lozano, G.; Bacher, G.; Beckers, T. Differential roles of p21(Aaf1) and p27(Kip1) in modulating chemosensitivity and their possible application in drug discovery studies. *Mol. Pharmacol.* **2001**, *60*, 900–906.
- Tahir, S. K.; Kovar, P.; Rosenberg, S. H. Rapid colchicine competition binding scintillation proximity assay using biotin-labeled tubulin. *BioTechniques* **2000**, *29*, 156–160.
- Bacher, G.; Bernd, N.; Peter, E.; Udo, V.; Siegfried, S.; Alexei, S.; Thomas, K.; Thomas, B. D-24851, a novel synthetic microtubule inhibitor, exerts curative antitumoral activity in vivo, shows efficacy toward multidrug-resistant tumor cells, and lacks neurotoxicity. *Cancer Res.* **2001**, *61*, 392–399.
- Mahboobi, S.; Pongratz, H.; Hufsky, H.; Hockemeyer, J.; Frieser, M.; Lyssenko, A.; Paper, D. H.; Bürgermeister, J.; Böhmer, F.-D.; Fiebig, H.-H.; Burger, A. M.; Baasner, S.; Beckers, T. Synthetic 2-arylidole derivatives as a new class of potent tubulin-inhibitory, antimetabolic agents. *J. Med. Chem.* **2001**, *44*, 4535–4553.
- Byth, K. F.; Culshaw, J. D.; Green, S.; Oakes, S. E.; Thomas, A. P. Imidazo[1,2-*a*]pyridines. Part 2: SAR and optimisation of a potent and selective class of cyclin-dependent kinase inhibitors. *Bioorg. Med. Chem. Lett.* **2004**, *14*, 2245–2248.
- Siebert, C. D. Arzneistoffentwicklung – Das Bioisosteriekonzept. *Chem. Unserer Zeit* **2004**, *38*, 320–324.
- Capdeville, R.; Buchdunger, E.; Zimmermann, J.; Matter, A. Glivec (STI571, imatinib), a rationally developed, targeted anticancer drug. *Nat. Rev. Drug Discovery* **2002**, *1*, 493–502.
- Kinet, J.-P.; Moussy, A. Use of tyrosin kinase inhibitors for treating cerebral ischemia. PCT WO 2004/096225 A2, 2004.
- Ciufolini, M.; Wermuth, C.; Gielthen, B.; Moussy, A. Preparation of 2-(3-aminoaryl)amino-4-aryl-thiazoles as tyrosin phosphokinase c-Kit inhibitors. PCT WO 2004/014903 A1, 2004.
- Beckers, T.; Reissmann, T.; Schmidt, M.; Burger, A. M.; Fiebig, H. H.; Vanhoefer, U.; Pongratz, H.; Hufsky, H.; Hockemeyer, J.; Frieser, M.; Mahboobi, S. 2-Arylidoles, a novel class of potent, orally active small molecule tubulin inhibitors. *Cancer Res.* **2002**, *62*, 3113–3119.
- O'Brian, J.; Wilson, I.; Orton, T.; Pognan, F. Investigation of the Alamar Blue (resazurin) fluorescent dye for the assessment of mammalian cell toxicity. *Eur. J. Biochem.* **2000**, *267*, 5421–5426.
- Ramsh, S. M.; Ginak, N. A.; Sochilin, E. G. Study of the reactivity and tautomerism of azolidines. XXVII. Study of 2-(arylimino)-thiazolidin-4-one tautomerism by UV and IR spectroscopy. *Zh. Org. Khim.* **1979**, *15*, 1506–1513.
- Pawar, R. A.; Rajput, A. P. Studies on the Vilsmeier–Haack reaction. A versatile new synthesis of 4-chloro-2-phenylaminothiazole-5-carboxaldehyde and related fused heterocyclic compounds and heterocyclic Schiff's bases. *Indian J. Chem., Sect. B: Org. Chem. Incl. Med. Chem.* **1989**, *28*, 866–867.
- Pohloudek-Fabini, R.; Schroepf, E. Acid isothiocyanates. III. Acid isothiocyanate conversion to unsymmetric, disubstituted acylthioureas with aromatic amines. 2. *Pharmazie* **1968**, *23*, 561–566.
- Pohloudek-Fabiani, R.; Schroepf, E. Acid isothiocyanates. III. Acid isothiocyanate conversion to unsymmetric, disubstituted acylthioureas with aromatic amines. 2. *Pharmazie* **1968**, *23*, 561–566.
- Rao, R. P. Thiazolidinones and thiazolidinediones as fungicidal agents. *Indian J. Appl. Chem.* **1960**, *23*, 110.
- Singh, A.; Uppal, A. S. Structure of acylated 4-aminothiazolines: Part XII. Studies in 4-aminothiazolines. *Indian J. Chem., Section B: Org. Chem. Incl. Med. Chem.* **1978**, *16*, 779–781.
- Ganapathi, K. Chemotherapy of bacterial infections. III. Synthesis of N4-amino-substituted heterocyclic derivatives of sulfanilamide. *Proc.—Indian Acad. Sci., Sect. A* **1940**, *12*, 278–283.

JM060545P